JOURNAL OF AGRICULTURAL AND FOOD CHEMISTRY

Influence of Complexation between Amylose and a Flavored Model Sponge Cake on the Degree of Aroma Compound Release

María-Ángeles Pozo-Bayon,[‡,§] Benoit Biais,[†,⊥] Vincent Rampon,[†] Nathalie Cayot,[‡] and Patricia Le Bail*,[†]

INRA, UBIA, rue de la Géraudière, B.P. 71627, F-44316 Nantes Cedex 3, France, and UMR no. 1129 FLAVIC, ENESAD, INRA, Université de Bourgogne, 17 rue Sully, B.P. 86510, F-21065 Dijon Cedex, France

Flavoring is used in the food industry to reinforce the aroma profile of baked cereal goods. During the processing of such products, interactions between starch and aroma compounds can occur, and this may have an impact on aroma release and perception. In the present study, 20 aroma compounds were tested to establish whether they formed complexes with amylose. The structure of the complexes was determined by wide-angle X-ray scattering (WAXS). A cocomplexation study proved that several complexing compounds could be present in the same crystalline aggregate. WAXS and differential scanning calorimetry (DSC) experiments were performed in a flavored model sponge cake at different steps of processing and showed that aroma compounds might form complexes with amylose in a sponge cake as they can do in simple system containing only amylose. Some of the aroma compounds trapped in the sponge cake were quantified, and their release behavior was followed by headspace analysis. The V-type structure could partly explain aroma retention in the product and the rate of aroma release.

KEYWORDS: Amylose/aroma compound complexes; wide-angle X-ray scattering; differential scanning calorimetry; dynamic headspace analysis; fluorescent spectroscopy

INTRODUCTION

The flavor of bakery products is the result of aroma compounds produced by enzymatic, fermentative, and thermal reactions during baking. Many aroma compounds initially present in the dough and others generated during baking could be lost by evaporation during processing. Flavoring of bakery goods is thus widely employed to compensate for this loss (*1, 2*) or to produce products with special aroma characteristics (*3*).

During baking, reactions and interactions could occur between aroma compounds and the different constituents of dough such as lipids, proteins, and starch. Depending on the affinity of the aroma compounds for the food matrix, the release of each aroma compound from the matrix will be different, and thus the amount of aroma compounds available for consumer's perception will be different too.

Baking is also one of the major factors affecting the texture of baked goods as it influences the structural evolution of starch. Moreover, it is known that the structure of starch is still changing after cooking, and that the different macromolecules of the starch granules have different behaviors. The modifications that starch undergoes depend on the different ingredients in the dough and mainly on the amount of water. The flavor compounds added to the dough in manufactured baked products may also play a role in the behavior of starch and be affected by the kind of food matrix (formulation, hydration, etc.). Specific interactions might occur depending on the morphology of the complex, which can be identified (*4, 5*).

During the cooking or baking process, starch granules swell, and amylose is leached out of the swollen starch granules. Some small molecules, such as aroma compounds or fatty acids, may then form amylose complexes (*6*). Amylose complexes with aroma compounds have been studied by several authors in simple systems (*4, 7–9*). Some studies were also conducted to determine the impact of these interactions on aroma release in more elaborate food matrixes (*8, 10, 11*).

The crystalline structure and thermostability of amylose complexes, commonly called "V type", are generally studied using X-Ray scattering and differential scanning calorimetry (DSC). Solid-state NMR (*12*), FT-IR, and Raman spectroscopy (*13–15*) have also been used to study these complexes. Depending on the complexing molecules, different types of $V_{amylose}$ have been described for linear alcohols (*16–19*), monoacyl lipids (*20, 21*),

* Corresponding author. Tel.: +33 240675054. Fax: +33 240675084. E-mail: patricia.le-bail@nantes.inra.fr.
† INRA.
‡ Université de Bourgogne.
§ Current affiliation: Instituto de Fermentaciones Industriales (CSIC). C/ Juan de la Cierva, 3, 28808, Madrid, Spain.
⊥ Current affiliation: INRA Bordeaux, UMR619 Fruit Biology, 71 ave Edouard Bourlaux, F-33883 Villenave d'Ornon Cedex, France.

10.1021/jf800242r CCC: $40.75
Published on Web 07/12/2008

Table 1. Aroma Compounds Present in the Flavoring Mixture and Behavior towards Amylose

aroma compound	CAS number	log P [a]	vapor pressure mmHg at 25 °C[b]	quantity added to the aroma formulation mg/L	amylose crystalline state
decanoic acid	334-48-5	4.02	0.00878	3	V_{6I} type
propylene glycol	57-55-6	−0.78	0.111	710 (solvent)	V_{6I} type
ethyl hexanoate	123-66-0	2.83	1.8	2	V_{6II} type
hexanoic acid	142-62-1	2.05	0.278	1	V_{6III} type
cis-3-hexen-1-ol	928-96-1	1.61	0.937	2	V_{6II} type
butyric acid	107-92-6	1.07	2.11	5	V_{6III} type
γ-decalactone	706-14-9	2.57	0.00512	10	V_{6III} type
δ-decalactone	705-86-2	2.57	0.00475	8	V_{6III} type
1,2-benzodihydropyrone (dihydrocoumarin)	119-84-6	0.97	0.00827	5	V_{6III} type
ethyl acetate	141-78-6	0.86	98.3	5	B type
3-hydroxybutan-2-one (acetoin)	513-86-0	−0.36	2	6	B type
ethyl butanoate	105-54-4	1.85	14.6	3	B type
butane-2,3-dione (diacetyl)	431-03-8	−1.34	70.2	3	B type
methyl cinnamate	103-26-4	2.36	0.0124	2	B type
2,5-dimethyl-4-hydroxy-2,3-dihydrofuran-3-one (furaneol)	3658-77-3	0.82	0.00058	10	B type
benzaldehyde	100-52-7	1.71	1.01	2	B type
2-methyl-3-hydroxy-4-pyranone (maltol)	118-71-8	−0.19	0.0000428	15	B type
citral	5392-40-5	3.45	0.0913	5	B type
5-(2-hydroxyethyl)-4-methylthiazole (sulfurol)	137-00-8	1.11	0.00171	3	B type
3-methoxy-4-hydroxybenzaldehyde (vanillin)	121-33-5	1.05	0.000447	200	B type

[a] Log P = log of the partition coefficient of the compound between water and octanol, calculated values from EPI estimation programs interface v3.20. [b] Estimated values from EPI estimation programs interface v3.20. The program estimates vapor pressure by three separate methods: the Antoine method, the modified Grain methods, and the Mackay method.

iodine (*22, 23*), dimethyl sulfoxide (*24*), potassium hydroxide (*25*), glycerol (*26*), and naphthol (*27*). Most $V_{amylose}$ structures are made from sixfold or, to a lesser extent eightfold, left-handed helices. They can therefore be classified into two families (V_6 and V_8) where 6 and 8 represent the number of D-glucosyl units per turn. In the V_6 family, three types of crystalline packing V_{6I}, V_{6II}, and V_{6III} (where I, II, and III define unit cells of different sizes) may be obtained depending on the nature of the complexing molecule. The complexing molecule can be trapped either in the single helix only (V_{6I} or V_h (*18*)) or both within and between amylose helices (V_{6II} or $V_{butanol}$ (*28*) and V_{6III} or $V_{2\text{-propanol}}$ (*29*)).

The aim of the present study is to establish if interactions between given aroma compounds and amylose may occur and if they could have an influence on a manufactured baked product flavored with these aroma compounds responsible for a "pastry" flavor. For that purpose, different model systems were studied going from the simplest one to a model sponge cake, quite similar to the manufactured product.

MATERIALS AND METHODS

Materials. Amylose was obtained from Sigma (France). It was a type III amylose extracted from potatoes. The degree of polymerization (DP) was determined by viscosimetry with a "CONTRAVES Low Shear 40" viscosimeter and found to be nearly 850.

Nineteen aroma compounds dissolved in propylene glycol, responsible for a "pastry" flavor, were analyzed. The aroma compounds are listed in **Table 1** together with their CAS number, their content in the flavoring mixture, and their behavior towards amylose. They were purchased from Sigma-Aldrich, and their purity was verified by GC−MS before use.

Sponge cake dough was made with wheat flour (type 55, used from the same batch), sucrose, pasteurized whole eggs (liquid), palm oil, and salt. All of these ingredients were purchased in a local supermarket.

Preparation of Amylose−Aroma Complexes. An amount of 200 mg of amylose was dispersed in 20 mL of water (1% (w/w)). After bubbling nitrogen through the solution for 10 min, it was heated to 160 °C in a glass tube with a screw cap for 45 min. In another tube, 0.5 mL of flavor compounds was added to 10 mL of water and then heated and mixed at 90 °C for 10 min. The amylose solution was cooled to 90 °C for 2 or 3 min, and then the aroma compounds were added and the mixture was roughly shaken for 2 min, then left in an oil bath, cooled to room temperature, and stored for 48 h. The mixture was centrifuged at 20 000*g* for 20 min at 20 °C, and the precipitates were conditioned by desorption of water by equilibration over saturated NaCl solution (aw = 0.7508).

Preparation of Sponge Cake Samples. *Dough Preparation.* Eggs, sucrose, and salt were mixed together with a household electric mixer in a water bath at 50 °C for 5 min. The resulting foam was removed from the water bath and mixed again for 2 min after 1 min of rest. Flour was then added little by little and gently incorporated into the foam with a wooden spoon. Melted palm oil was added and gently stirred into the mix. To flavor the sponge cake dough, the formulated aroma was added to the melted palm oil. The flavored oil was added to the foamed dough to obtain a 1% (w/w) aromatized dough.

Baking. The dough (210 g) was placed in a Teflon-coated aluminum mold (25 cm × 10 cm) and baked in a household electric oven for 25 min at 195 °C.

Sampling and Storage. After baking, the cakes were immediately removed from the molds and left to cool at room temperature. The crust was then removed, and crumb was used for the wide-angle X-ray scattering (WAXS) measurements. Crumb was either used immediately for X-ray diffraction measurements (fresh sponge cake) or left to equilibrate at 75% relative humidity by desorption over a saturated NaCl solution (aw = 0.75 at 25 °C). Crumb stored in such conditions was sampled between 24 and 144 h to study the influence of ageing on starch retrogradation.

Wide-Angle X-ray Scattering. About 50 mg of sample was sealed in a copper ring between two scotch tape sheets to prevent any change in water content and examined by WAXS with an Inel diffractometer (Inel, France), operating at 40 kV and 30 mA with a Cu $K\alpha_1$ radiation (0.15405 nm) provided by a quartz monochromator. Data were monitored by a 120° curve detector (CPS 120−Inel, France) for 2 h and normalized between 3° and 30° (2θ). Samples were made up as follows: the constituents were put into a flask and mixed with a spoonbill; the mixture was then removed using a micropipette with a conical nozzle.

Differential Scanning Calorimetry. DSC thermograms were recorded using an automated heat flux differential scanning calorimeter SETARAM DSC 121 (France). Stainless steel high-pressure pans were used. The system was calibrated with indium, and a pan containing 100 μL of water was taken as reference. All of the different constituents were mixed together in the DSC pan. They were weighed according to

Table 2. Ingredients and Their Content for the Different Models Studied by DSC (g for 100 g)

ingredients	flour	palm oil	salt	sucrose	water
cell 1	65.0				35.0
cell 2	62.5		2.5		35.0
cell 3	56.0	9.0			35.0
cell 4	32.5			32.5	35.0
cell 5	31.9		1.2	31.9	35.0
cell 6	29.6	4.7	1.1	29.6	35.0

the order indicated in **Table 2**. After crimping, the pan was centrifuged twice (1800*g* for 3 min). The pan was turned over between the two centrifugations. Two successive scans were run at 2 °C/min between 5 and 150 °C, separated by a cooling stage at about 10 °C/min (in order to obtain a better comparison between thermograms).

Fourier Transform Infrared Spectroscopy. Infrared spectra were recorded on a Fourier transform infrared (FT-IR) spectrometer Vector 22 (Bruker, France). The samples were prepared as KBr pellets. For each experiment, 2 mg of sample was mixed with 100 mg of KBr and die-cast at 300 kg/cm^2. Spectra were obtained in the transmission mode between 2000 and 800 cm^{-1} at 4 cm^{-1} interval. They were baseline-corrected and normalized (OPUS software, v2.06). Spectral data were analyzed by applying principal component analysis (PCA) as reported by Robert et al. (*31*). The use of PCA reveals the most significant absorption bands that have changed. The principal component scores of standard mixtures were used to asses prediction equations, whereas principal component scores of amylose complexes made it possible to determine the amount of ligand trapped in the complexes.

Fluorescent Spectroscopy. Fluorescent spectroscopy was used to quantify 3-methoxy-4-hydroxybenzaldehyde (vanillin) and 1,2-benzodihydropyrone (dihydrocoumarin) fluorophors in the fresh dough and in the corresponding baked sponge cake. About 500 mg of the product was ground in 10 mL of ethanol. The mixture was stirred for 5 min and then filtered through a 0.45 μm poly(tetrafluoroethylene) filter. Five milliliters of the filtrate was diluted in 5 mL of pure water before analysis. For dihydrocoumarin, the filtrate was diluted to 1/20 in an ethanol/water mixture (50/50 (v/v)). Right-angle steady-state fluorescence measurements were done on these diluted filtrates with a Hitachi F-4500 FL spectrofluorimeter. The samples were measured in a quartz cell. For vanillin, the excitation wavelength was set at 355 nm and the emission spectrum was measured from 365 to 480 nm at 240 nm/min. For dihydrocoumarin, the excitation wavelength was set at 275 nm and the emission spectrum was measured from 285 to 350 nm at 240 nm/min. Quantities were determined from calibration curves that were obtained with solutions of known concentrations of both compounds.

Dynamic Headspace Gas Chromatography Analysis of the Sponge Cake. This technique was used to follow the release of volatile compounds from the sponge cake model. An amount of 20 g of cake sample was placed in a 500 mL glass vessel inside a water bath at 25 °C. The headspace was purged by N_2 at 25 mL/min for a given duration. The gas phase containing the aroma compounds was trapped in a capillary glass tube (3 mm i.d.) containing about 100 mg of Tenax adsorbent. A new sample was used for each purge step. The desorption and the quantification of the aroma compounds trapped on the Tenax adsorbent was measured on a Hewlett-Packard (Palo Alto, CA) 5890 series II gas chromatograph, equipped with a Chrompack TCT/PTI 400 injector. The injection parameters were as follows: precooling of glass trap −160 °C, 4 min; desorption, 10 min at 250 °C with a helium flow of 20 mL/min; finally flash injection at 250 °C. The gas chromatograph was equipped with a flame ionization detector at 250 °C. An inactivated fused-silica precolumn (30 cm × 0.25 mm i.d.) and a fused-silica capillary column (30 m long, 0.25 mm i.d., and 0.5 μm film thickness) coated with a stationary phase DB-Wax (J & W Scientific, U.S.A.) were used. Helium was used as the carrier gas, and the chromatographic temperature was programmed from 40 °C (maintained for 5 min) to 250 °C at a rate of 4 °C/min, with a final isotherm of 15 min. After each analysis, the Tenax tube was reconditioned for 2 h in an oven (280 °C) with a nitrogen flow (80 mL/min). Different purge times were used from 5 min to 14 h. Aroma release analyses were done in triplicate.

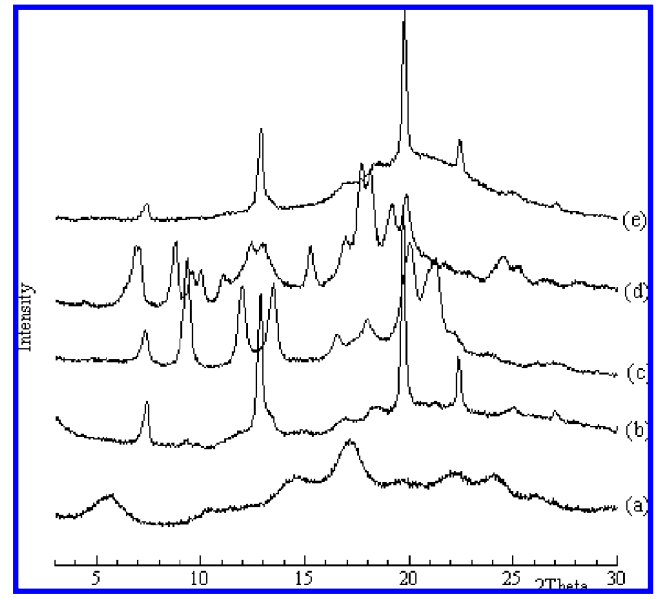

Figure 1. X-rays diffractograms obtained for amylose dispersion crystallized with addition of furaneol (**a**), propylene glycol (**b**), *cis*-3-hexen-1-ol (**c**), γ decalactone (**d**), and "pastry" aroma (**e**).

The results are expressed as the percentage of aroma release compared to the release obtained after 14 h of purge.

RESULTS AND DISCUSSION

At first, to establish the capability of each aroma compound from the "pastry" aroma to form complexes with the amylose, a protocol of amylose in vitro crystallization was developed in temperature conditions close to the sponge cake baking temperature. Each sample obtained was studied by X-ray diffraction. Since Rutschmann and Solms (*5*) and Arvisenet et al. (*30*) highlighted the fact that competition phenomena can occur when several flavoring molecules are in contact with amylose, we studied competition towards amylose between two complexing aroma compounds (one complexing in V_{6I}-type structure and the other in a structure containing space between helices, for example, V_{6II} or V_{6III}).

In the second step, DSC analyses were done on each different ingredient of the sponge cake. Ingredients were analyzed one by one, and then in the whole recipe mixture for the sponge cake dough. X-ray diffraction was also performed to check the formation of amylose−aroma complexes in the sponge cake during baking.

Finally, to verify the hypothesis that the type of complexes formed during thermal treatment of starch may influence the amount of aroma trapped, and therefore the aroma compounds available for release, the volatile compounds trapped in the sponge cake were quantified and aroma release was followed by dynamic headspace analysis.

1. Interactions between Amylose and Aroma Compounds. *Specific Interactions between Amylose and Aroma Compounds Added One by One.* The complexing ability of each flavor compound was studied with pure amylose. Complexes were obtained as described in the Materials and Methods section, and they were studied by WAXS. From the 20 compounds of the flavoring formulation, only 9 formed complexes with amylose. The diagram obtained with furaneol (**Figure 1a**) was characteristic of B amylose and, thus, related to the retrogradation of amylose without any complexes (*32, 33*). The X-ray diffraction pattern on amylose with propylene glycol (**Figure 1b**) showed five reflections at 2 = 7.4°, 12.9°, 19.8°, and 22.4° (λ = 0.15405

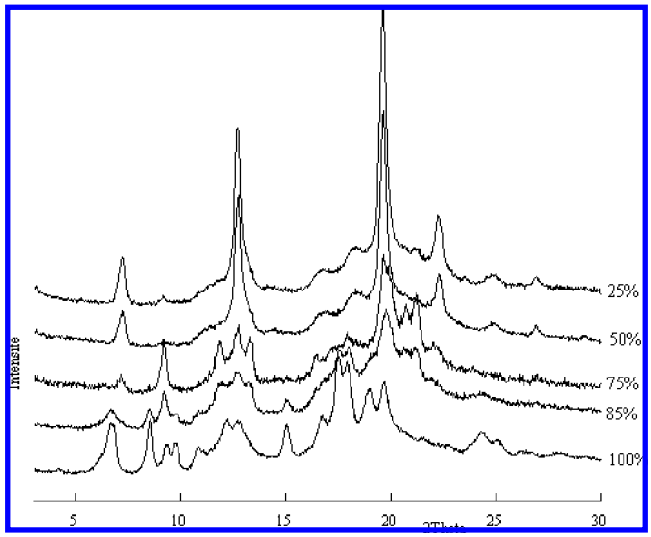

Figure 2. X-ray diffractograms of amylose decanoic acid−δ-decalactone complexes. The percentage of δ-decalactone is indicated on the curve (decanoic acid was added up to 100%).

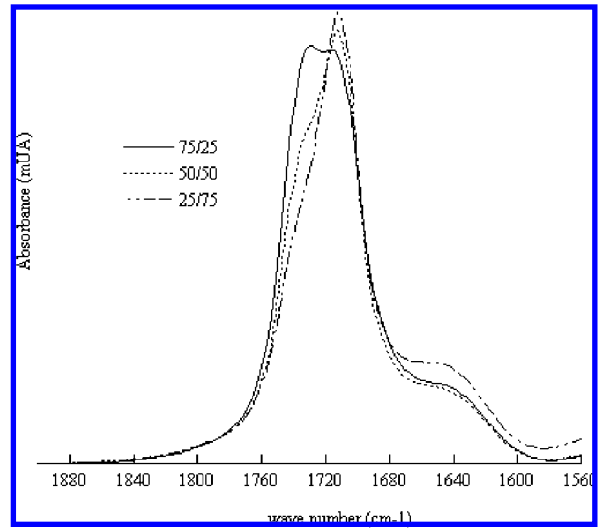

Figure 3. FT-IR spectra of decanoic acid−δ-decalactone complexes (δ-decalactone/decanoic acid proportion).

nm), all of which are characteristics of the V_{6I} polymorph of amylose. The precipitation of amylose in the presence of *cis*-3-hexen-1-ol led to the formation of V_{6II} complexes. The corresponding diagram (**Figure 1c**) showed reflections at $2\Theta = 7.3°$, 9.4°, 12°, 13.4°, 16.5°, 18°, 20°, 20.8°, 21.12°, and 22.1° ($\lambda = 0.15405$ nm). The reflections obtained for γ-decalactone (**Figure 1d**) with amylose at $2\Theta = 6.9°$, 8.8°, 9.6°, 10.0°, 11.1°, 12.5°, 13.0°, 15.2°, 17°, 18.1°, 19.2°, 19.9°, 24.5°, and 25.2° ($\lambda = 0.15405$ nm) are characteristics of the V_{6III}-type structure.

The complexing ability for all the flavor compounds is shown in **Table 1**. As often reported in the literature, it can be observed that the complexing ability was strictly dependent on neither the chemical class of the compound nor the hydrophobicity (log *P*). Among the three esters, only one (ethyl hexanoate) formed complexes. The two ketones also formed complexes with amylose, but the two aldehydes did not. Among the alcohols, only propylene glycol and *cis*-3-hexen-1-ol formed complexes. Log *P* values of complex forming molecules varied from −0.78 to 2.83. Some highly hydrophobic compounds such as citral did not form complexes, whereas others such as ethyl hexanoate did.

Among the compounds that formed complexes, different types of crystalline polymorph (V_{6I}, V_{6II}, or V_{6III}) were observed (**Table 1**). **Figure 1e** shows a V_{6I}-type structure for the complex amylose−"pastry" aroma. This result can show the influence of propylene glycol, which was found to be a complexing agent (V_{6I} polymorph). It is used as solvent and therefore present in large quantities in the flavoring mixture.

Competition between Aroma Compounds in Complexation with Amylose. To determine the effect of the presence of several aroma compounds in the mixture on complexation with amylose, a cocomplexation study was made. Different mixtures of decanoic acid (V_{6I}-type complexes) and δ-decalactone (V_{6III}-type complexes) were used to make complexes with amylose as described in the Materials and Methods section. **Figure 2** shows the X-ray diagrams of the complexes obtained for the aroma mixtures containing between 25% (m/m) and 100% of δ-decalactone (the mixtures were completed with decanoic acid). Up to 50% δ-decalactone did not modify the crystalline packing, and the diagram obtained was identical to that with decanoic acid (V_{6I}). Beyond this proportion (75% and 85% of δ-decalactone), the presence of both aroma compounds induced spacing between the helices and the crystalline packing was a V_{6II} structure.

For the complexes prepared with the mixture containing 75% of δ-decalactone, mathematical combinations of X-ray diagrams of V_{6I} and V_{6II} packing were done in order to obtain a theoretical spectrum close to what was observed. This combination highlighted the joint presence of V_{6I} and V_{6II} types in ratios 0.2 and 0.8, respectively, in this sample. Similar combinations were obtained with the mixture which contained 85% of δ-decalactone and showed the presence of V_{6I}, V_{6II}, and V_{6III} crystallites in the ratios 0.1, 0.5, and 0.4, respectively.

This study points out the occurrence of competition phenomena between ligands. Decanoic acid, which presented a stronger affinity to amylose, was predominantly included within the amylose helix, but when the proportion of δ-decalactone increased, it could also be trapped between helices, thus inducing inflation of the crystalline unit leading to the formation of V_{6II} and then V_{6III} types.

Figure 3 shows the infrared spectra (spectral area of the carbonyl functions for both aroma compounds) of the different complexes obtained with the mixtures decanoic acid/δ-decalactone. The spectrum obtained with the 75% δ-decalactone mixture showed two absorption bands, the first at 1706 cm^{-1} corresponding to the carbonyl function of decanoic acid and the second band at 1740 cm^{-1} which is characteristic of the carbonyl function of δ-decalactone. This proved that both compounds were present in the amylose complexes. Though the mixtures at 25% and 50% of δ-decalactone led to V_{6I}-type structures, the infrared spectra showed a shoulder at 1740 cm^{-1} which indicates the presence of δ-decalactone. The two aroma compounds were thus present in the V_{6I} complex too. Brisson et al. (*18*) reported that, in the V_{6I} packing, the complexing molecules could only be entrapped in the cavity of the helix. Nevertheless, our results suggest that in complexes obtained with the mixtures at 25% and 50% of δ-decalactone, the δ-decalactone molecule was also located in the helicoidal cavity. In fact, Biais (*34*) demonstrated by molecular modeling that depending on the conformation of the molecule, δ-decalactone can be included inside the cavity of the amylose helix.

These cocomplexation experiments showed that the presence of several complexing molecules in a mixture did not prevent complexation with amylose and that several complexing compounds could be present in the same crystalline aggregate.

Table 3. Parameters Characterizing the Release at Different Times of the Flavoring Compounds[a]

compound	relative release for different purge times mean ± SD				analysis of variance: effect of purge time on relative release
	5 min	15 min	30 min	60 min	*p*-values
ethyl butanoate	2.9 ± 1.5 a	12.7 ± 5.2 b	14.3 ± 5.8 b	28.6 ± 5.9 c	0.0007
ethyl hexanoate	0.5 ± 0.0 a	2.6 ± 0.5 b	4.9 ± 1.0 c	10.3 ± 0.8 d	$p < 0.0001$
methyl cinnamate	0.2 ± 0.3 a	1.2 ± 0.4 a	4.2 ± 0.2 a	7.3 ± 0.7 b	0.0030
3-methoxy-4-hydroxybenzaldehyde (vanillin)	5.5 ± 6.2	4.1 ± 4.4	4.7 ± 1.9	8.1 ± 6.1	0.7438
citral	0.7 ± 1.1 a	0.6 ± 1.1 a	2.9 ± 0.3 a	8.6 ± 2.3 b	0.0002
3-hydroxybutan-2-one (acetoin)	0.1 ± 0.1 a	1.5 ± 1.1 a	5.0 ± 0.4 b	9.9 ± 2.2 c	$p < 0.0001$
1,2-benzodihydropyrone (dihydrocoumarin)	48.5 ± 7.2	42.4 ± 22.5	56.3 ± 24.6	69.7 ± 60.4	0.8177
cis-3-hexen-1-ol	0.5 ± 0.0 a	2.1 ± 0.5 b	4.6 ± 0.8 c	10.3 ± 0.8 d	0.0000
propylene glycol	0.0 ± 0.0	0.1 ± 0.0	0.3 ± 0.2	0.2 ± 0.1	0.0856

[a] NB: For each volatile compound, different letters denote a statistically significant difference ($p < 0.0050$).

Additionally, due to competition effects, different proportions of the complexing molecules could induce intermediate crystalline types.

2. Formation of Amylose−Aroma Compound Complexes in Sponge Cake during Processing. The formation of amylose−aroma compound complexes in model sponge cake was followed at different steps during processing (before baking, during baking, immediately after baking, and during ageing).

Structural Study before Baking. The X-ray diffractogram corresponding to the sponge cake dough was quite similar to the diffractogram corresponding to the flour/water mixture at 35% (w/v), which corresponds to the water content determined in the sponge cake. X-ray diffractograms of the 35% flour/water mixture and of the sponge cake dough (data not shown) revealed predominantly A crystalline type, corresponding to the cereal starch pattern, with values of 2Θ equal to 9.9°, 11.2°, 15°, 17°, 18.1°, and 23.3°, and B crystalline type (5.6°, 15°, 17°, 22°, and 24°) in minor percentage.

The peak at 2Θ = 20° showed that there was another crystalline type present in the starch corresponding to a V crystalline type that might be the result of amylose−endogenous lipid complexes formed in the course of the hydrothermal treatments applied during flour extraction.

The other ingredients of the sponge cake, like palm oil and egg, showed central diffusion for 2Θ between 10° and 25° (data not shown), making the interpretation of the diagrams more difficult. As a consequence, the sponge cake diffraction spectrum was less well-defined than the spectrum of the flour/water mixture. It should be pointed out that the diffractogram of the nonflavored sponge cake dough and the spectrum of the flavored (1%) sponge cake dough were quite similar. To be sure that no amylose/palm oil complexes were being produced, the structure of palm oil−amylose mixtures was studied by X-ray scattering. The X ray diffraction diagram presented a B crystalline type (data not shown) confirming that palm oil did not interact with amylose.

During Baking (DSC). **Figure 4** shows the DSC thermograms from the different mixtures of the sponge cake constituents. The composition of the different mixtures is shown in **Table 2**.

The DSC thermal curves of wheat flour at high water levels (>60−70% water) showed a single endotherm at about 60 °C (data not shown). When water content decreased, two endothermic transitions became obvious. This behavior is typical of many granular starches studied by DSC (*35–37*), and it can be observed in **Figure 4a**, where the DSC thermal profile for wheat flour (35% water content) exhibited endotherms at both 60 and 86 °C. The presence of amylose−lipid complexes in starch systems was revealed by endothermic transitions at temperatures

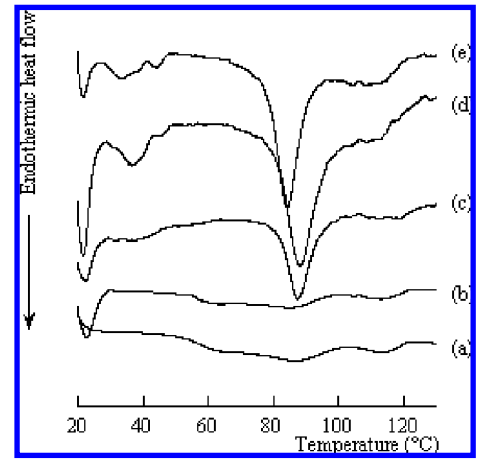

Figure 4. DSC thermograms: (**a**) flour−water (35%), (**b**) flour−palm oil−water, (**c**) flour−salt−sucrose−palm oil−water, (**d**) nonflavored sponge cake dough, and (**e**) flavored sponge cake dough (1%).

well above the melting endotherms of starch crystallite (95−130 °C), at 114 °C in **Figure 4a**. Amylose−lipid complexation, involving endogenous lipids, occurred during gelatinization of starch. The exothermic effect of complex formation was superimposed on the melting transition of starch crystallites (*38*).

Figure 4b shows the DSC thermal curves of the wheat flour−palm oil−water mixture (cell 3 in **Table 2**). Before reaching 50 °C, the endotherms were due to the palm oil melting. The thermogram was quite similar to the one corresponding to the (35%) flour−water mixture. The amylose−complex melting enthalpies were calculated on the basis of the quantity of flour present in the sample, $\Delta H_{(\text{flour-water})}$ and $\Delta H_{(\text{flour-palm oil-water})}$, and were, respectively, 3.8 J/g of flour and 3.3 J/g of flour. These values show that palm oil does not prevent complexation of endogenous lipids with amylose.

Figure 4c illustrates the thermal profiles of mixtures containing sucrose, salt, and palm oil. For all these samples, the gelatinization temperature was higher than that of the flour−35% water mixture. This phenomenon can be attributed to sugar and salt solvatation, which produces competition between starch, sugar, salt, and water. The endotherm due to the melting of amylose−endogenous lipid complexes was always present showing that the formation of these complexes was not much modified by sugar, salt, or palm oil.

Figure 4, parts **d** and **e**, shows the melting thermograms obtained upon heating nonflavored or flavored (1%) sponge cake dough. The DSC curves of the sponge cake dough contained many endotherms. Below 50 °C, the endotherms were due to the palm oil melting. From these curves, it was obvious that gelatinization started at about 65 °C and finished at 100 °C. The characteristic melting endotherm of the amylose complexes

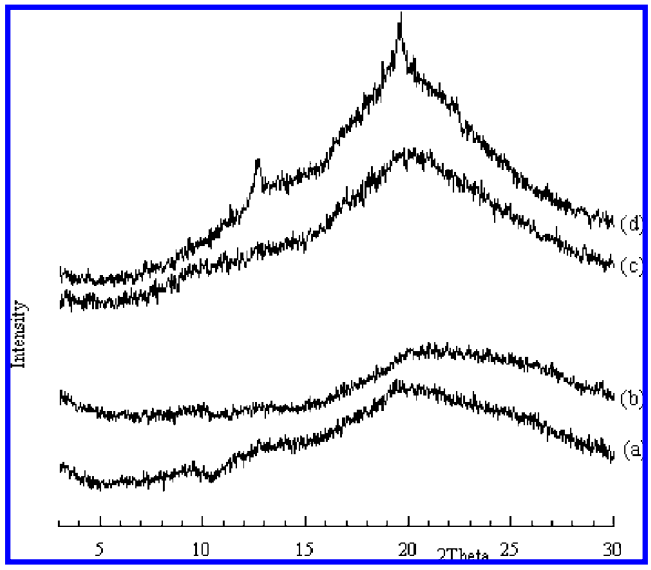

Figure 5. X-ray diffractograms: (**a**) nonflavored sponge cake crumb, (**b**) flavored sponge cake crumb, (**c**) nonflavored sponge cake crumb stored for 72 h at aw = 0.75, and (**d**) flavored sponge cake crumb stored for 72 h at aw = 0.75

was observed around 101 °C for the flavored sponge cake. As wheat starch contains lipids, the same endotherm also occurred for the nonflavored sponge cake dough. The complexity of this food matrix did not allow us to determine the origin of the complexes with amylose, that is to say, whether they were due to the endogenous lipids and/or to the flavoring compounds.

Immediately after Baking and during Ageing. The WAXS study performed on the cake crumbs after baking revealed that gelatinization of starch during baking was incomplete. Indeed, the X-ray diffractograms of the nonflavored and flavored (1%) sponge cakes (**Figure 5**, parts **a** and **b**) revealed residual peaks of the A crystalline type with values of 2Θ equal to 9.9°, 15°, and even a barely detectable peak at 5.6° confirming the presence of the B crystalline type.

In contrast with the evolution of the X-ray diffractograms of the nonflavored sponge cake crumb (**Figure 5c**), peaks of the V crystalline type appeared during the ageing of the flavored sponge cake crumb (**Figure 5d**). These results suggest that aroma compounds might form complexes with amylose in an elaborate food matrix like a sponge cake as they do in a simple system containing only amylose.

3. Aroma Compounds Trapped in the Sponge Cake. Some of the aroma compounds trapped in the sponge cake were quantified, and the release behavior of some was also followed by headspace analysis.

Quantification of Aroma Compounds Trapped in the Sponge Cake by Fluorescent Spectroscopy. The natural fluorescence of vanillin and dihydrocoumarin allow us to quantify them in the dough and in the sponge cake using fluorescence spectroscopy. Maximal emission and excitation wavelengths were found to be $\lambda_{excitation} = 343$ nm, $\lambda_{emission} = 388$ nm and $\lambda_{excitation} = 281$ nm, $\lambda_{emission} = 300$ nm for vanillin and dihydrocoumarin, respectively. These wavelengths were used for the quantification. It is noticeable that the fluorescence of vanillin was very sensitive to the solvent used (an increase in fluorescence was observed when ethanol was added to water to solubilize vanillin). Moreover, the fluorescence of dihydrocoumarin was shifted after complexation with amylose. A modification of the immediate molecular environment could explain this result. This phenomenon could be used to highlight the ability of dihydrocoumarin to form complexes with amylose. Calibration curves exhibited a linear correlation between fluorescence and the amount of molecule in the extracts with a correlation coefficient $r = 0.986$ and 0.964 for vanillin and dihydrocoumarin, respectively (data not shown).

Fluorescence due to vanillin and dihydrocoumarin was measured in the extracts of the dough and of the sponge cake. It was verified by front face setting that the residues obtained after extraction with ethanol were no longer fluorescent. The ethanol thus extracted all of the vanillin and dihydrocoumarin from the samples. The data were expressed as the percentage of aroma compound in the sample as compared to the amount of aroma compound added to the dough. The percentages of vanillin and dihydrocoumarin in the dough were 41% and 59%, respectively, whereas in the sponge cake it was 28% for vanillin and 54% for dihydrocoumarin. These results show that almost half of the aroma compounds were lost during the preparation of the dough. Some losses may be due to the volatility of the aroma compounds but also to their chemical reactivity as is the case with vanillin (possible reaction with egg proteins (*39*) or the formation of hemiacetal from alcohol and vanillin). These results also show that the loss of aroma compounds during baking was larger for vanillin (B-type amylose) than for dihydrocoumarin (V_{6III}-type amylose), even though vanillin is less volatile than dihydrocoumarin.

Release of Aroma Compounds from the Flavored Sponge Cake. Dynamic headspace analysis was performed with different purge times (5, 15, 30, 60 min and 14 h). These long times were chosen in order to evaluate the release of volatile compounds during the storage of a sponge cake. Additionally, the cakes were crushed in order to accelerate the phenomena occurring during storage. In order to compare the rate of release for each compound of the flavoring mixture, data were expressed as relative percentages of the peak area measured for the 14 h purge. These results are shown in **Table 3**. The huge standard deviations found for some aroma compounds may be attributed partly to the fact that sponge cake samples were crushed resulting in irregular exchange surfaces for the mass transfer of volatiles. Only very small quantities of some of the compounds were extracted from the cakes, which resulted in small peaks and induced large standard deviations. The ANOVA procedure was used to check the significance of increases in aroma release as a function of time. The results are also reported in **Table 3**.

Most of the aroma compounds showed an increase in release with an increase in the purge time. Nevertheless, the release of vanillin, dihydrocoumarin, and propylene glycol did not follow this trend. Moreover, propylene glycol and dihydrocoumarin exhibited extremely different behaviors: hardly any propylene glycol was released into the headspace, whereas a large proportion of dihydrocoumarin was released from the first 5 min of purge.

Within one chemical class, ethyl butanoate showed higher release than did ethyl hexanoate. This could be explained by the higher volatility of ethyl butanoate compared with ethyl hexanoate. Another possible explanation is the greater ability of ethyl hexanoate to form complexes with amylose, which could have favored its retention in the cake and thus limited its release. Pozo-Bayon et al. (*40*) showed that the release of this compound was not affected by changes in the lipid composition of the cakes (as is the case for compounds with similar physicochemical properties) suggesting that interactions with some dough ingredients could be taking place.

The *cis*-3-hexen-1-ol exhibited the same release rate as that of ethyl hexanoate. Both are able to form V_{6II} amylose

complexes. The strong retention of propylene glycol cannot be entirely explained by its physicochemical properties; it is also likely that it can form V_{6I} complexes with amylose.

Considering the data reported in **Table 3**, it is noticeable that, in spite of their ability to form complexes, the release trend of *cis*-3-hexen-1-ol and ethyl hexanoate did not greatly differ from the release of other noncomplexing compounds with similar physicochemical properties (e.g., methyl cinnamate). Dihydrocoumarin and vanillin were quickly released into the headspace, and their release was not increased with purge time, suggesting that these compounds were very feebly retained by the cake. The ability of dihydrocoumarin to form V_{6III} complexes did not seem to increase the retention of this compound, which was the least retained of all of them.

These results suggest that it is not only the capacity of some aroma compounds to form complexes with amylose that could affect aroma release from model sponge cake but also the type of polymorphism could determine the extent of this effect.

ACKNOWLEDGMENT

We thank Bruno Pontoire and Paul Robert for helpful discussion and assistance in performing X-ray and IR measurements.

LITERATURE CITED

(1) De Roos, J. J.; Mansecal, R. Poor performance of flavouring in heat processed products: a problem of poor flavor retention or poor release? In *Flavour Research at Dawn of Twenty First Century*; Le Quéré, J. L., Etievant, P. X., Eds; Lavoisier: Paris, France, 2003; pp 27−32.

(2) Pozo-Bayon, M.; Guichard, E.; Cayot, N. Feasibility and application of solvent assisted flavour evaporation and standard addition method to quantify the aroma compounds in flavoured baked matrices. *Food Chem*. **2006**, *99*, 416–423.

(3) Pszczola, D. E. 50 Ingredient hot spots highlighted. *Food Technol.* **2002**, *56*, 32–50.

(4) Rutschmann, M. A.; Solms, J. Formation of inclusion complexes of starch in ternary model systems with decanal, menthone and 1-naphtol. *Lebensm.-Wiss. Technol*. **1990**, *23* (5), 457–464.

(5) Rutschmann, M. A.; Solms, J. Formation of inclusion complexes of starch with different organic compounds. V. Characterization of complexes with amperometric iodine titration, as compared with direct quantitative analysis. *Lebensm.-Wiss. Technol*. **1990**, *23*, 88–93.

(6) Fanta, G. F.; Shogren, R. L.; Salch, J. H. Stream jet cooking of high-amylose starch−fatty acid mixtures. An investigation of complex formation. *Carbohydr. Polym*. **1999**, *38*, 1–6.

(7) Nuessli, J.; Putaux, J. L.; Le Bail, P.; Buléon, A. Crystal structure of amylose complexes with small ligands. *Int. J. Biol. Macromol*. **2003**, *33*, 227–234.

(8) Nuessli, J.; Sigg, B.; Conde-Petit, B.; Escher, F. Characterization of amylose−flavour complexes by DSC and X-ray diffraction. *Food Hydrocolloids* **1997**, *11*, 27–34.

(9) Heinemann, C.; Escher, F.; Conde-Petit, B. Structural features of starch−lactone inclusion complexes in aqueous potato starch dispersions: the role of amylose and amylopectin. *Carbohydr. Polym*. **2003**, *51*, 159–168.

(10) Arvisenet, G.; Le Bail, P.; Voilley, A.; Cayot, N. Influence of physicochemical interactions between amylose and aroma compounds on the retention of aroma in food-like matrices. *J. Agric. Food Chem*. **2002**, *50*, 7088–7093.

(11) Heinemann, C.; Conde-Petit, B.; Nuessli, J.; Escher, F. Evidence of starch inclusion complexation with lactones. *J. Agric. Food Chem*. **2001**, *49*, 1370–1376.

(12) Le Bail, P.; Rondeau, C.; Buléon, A. Structural investigation of amylose complexes with small ligands: helical conformation, crystalline structure and thermostability. *Int. J. Biol. Macromol*. **2005**, *35*, 1–7.

(13) Cael, J. J.; Koenig, J. L.; Blackwell, J. Infrared and Raman spectroscopy of carbohydrates. Part VI: Normal coordinate analysis of V-amylose. *Biopolymers* **1975**, *14*, 1885–1903.

(14) Biais, B.; Le Bail, P.; Robert, P.; Buleon, A. Localisation et dosage de composés d'arômes dans des matrices amylacées en milieu concentré. *Ind. Cereales* **2005**, *142*, 17–20.

(15) Biais, B.; Le Bail, P.; Robert, P.; Pontoire, B.; Buleon, A. Structural and stoichiometric studies of complexes between aroma compounds and amylose. Polymorphic transitions and quantification in amorphous and crystalline areas. *Carbohydr. Polym*. **2006**, *66*, 306–315.

(16) Buléon, A.; Duprat, F.; Booy, F. P.; Chanzy, H. Single crystals of amylose with a low degree of polymerisation. *Carbohydr. Res*. **1984**, *4*, 161–173.

(17) Whittam, M. A.; Orford, P. D.; Ring, S. G.; Clark, S. A.; Parker, M. L.; Cairns, P.; Miles, M. J. Aqueous dissolution of crystalline and amorphous amylose−alcohol complexes. *Int. J. Biol. Macromol*. **1989**, *11*, 339–344.

(18) Brisson, J.; Chanzy, H.; Winter, W. T. The crystal and molecular structure of Vh amylose by electron diffraction analysis. *Int. J. Biol. Macromol*. **1991**, *13*, 31–39.

(19) Le Bail, P.; Bizot, H.; Pontoire, B.; Buléon, A. Polymorphic transitions of amylose−ethanol crystalline complexes by moisture exchanges. *Starch/Staerke* **1995**, *47*, 229–232.

(20) Godet, M. C.; Tran, V.; Delage, M. M.; Buléon, A. Molecular modelling of the specific interactions involved in the amylose complexation by fatty acids. *Int. J. Biol. Macromol*. **1993**, *15*, 11–16.

(21) Godet, M. C.; Bizot, H.; Buléon, A. Crystallization of amylose−fatty acid complexes prepared with different amylose chain lengths. *Carbohydr. Polym*. **1995**, *27*, 47–52.

(22) Bluhm, T. L.; Zugenmaier, P. Detailed structure of the Vh−amylose−iodine complex: a linear polyiodine chain. *Carbohydr. Res*. **1981**, *89*, 1–10.

(23) Yu, X.; Houtman, C.; Atalla, R. H. The complex of amylose and iodine. *Carbohydr. Res*. **1996**, *292*, 129–141.

(24) Winter, W. T.; Sarko, A. Crystal and molecular structure of the amylose−DMSO complex. *Biopolymers* **1974**, *13*, 1461–1482.

(25) Sarko, A.; Biloski, A. Crystal structure of the KOH−amylose complex. *Carbohydr. Res*. **1980**, *79*, 11–21.

(26) Hulleman, S. H. D.; Helbert, W.; Chanzy, H. Single crystals of V amylose complexed with glycerol. *Int. J. Biol. Macromol*. **1996**, *18*, 115–122.

(27) Yamashita, Y.; Monobe, K. Single crystals of amyloseV complexes. II. Crystals with 81 helical configuration. *J. Polym. Sci*. **1971**, *9*, 1471–1481.

(28) Helbert, W.; Chanzy, H. Single crystals of V amylose complexed with *n*-butanol or *n*-pentanol: structural features and properties. *Int. J. Biol. Macromol*. **1994**, *16*, 207–213.

(29) Buléon, A.; Delage, M. M.; Brisson, J.; Chanzy, H. Single crystals of V amylose complexed with isopropanol and acetone. *Int. J. Biol. Macromol*. **1990**, *12*, 25–33.

(30) Arvisenet, G.; Voilley, A.; Cayot, N. Retention of aroma compounds in starch matrices: competitions between aroma compounds toward amylose and amylopectin. *J. Agric. Food Chem*. **2002**, *50*, 7345–7349.

(31) Robert, P.; Devaux, M.-F.; Bertrand, D. Beyond prediction: extracting relevant information from near infrared spectra. *J. Near Infrared Spectrosc*. **1996**, *4*, 75–84.

(32) Hibi, Y.; Kitamura, S.; Kuge, T. Effect of lipids on the retrogradation of cooked rice. *Cereal Chem*. **1990**, *67*, 7–10.

(33) Bulkin, B. J.; Kwask, Y. Retrogradation kinetics of waxy corn and potato starches a rapid raman spectroscopic study. *Carbohydr. Res*. **1987**, *160*, 95–112.

(34) Biais, B. Etude structurale et mécanismes de formation de complexes amylose−ligand. influence sur la rétention de composés d'arôme dans une matrice amylacée. Ph.D. Dissertation, Nantes University, Nantes, France, 2006.

(35) Donavan, J. W. Phase transition of the starch−water system. *Biopolymers*. **1979**, *18*, 263–275.

(36) Biliaderis, C. G. Structures and phases transitions of starch in food systems. *Food Technol.* **1992**, 98–145.
(37) Fukuoka, M.; Ohta, K. I.; Watanbe, H. Determination of the terminal extent of starch gelatinization in a limited water system by DSC. *J. Food Eng.* **2002**, *53*, 39–42.
(38) Biliaderis, C. G.; Page, C. M.; Maurice, T. J. Non-equilibrium melting of amylose-V complexes. *Carbohydr. Polym.* **1986**, *6*, 269–288.
(39) Grinberg, V. Y.; Grinberg, N. V.; Mashkevich, A. Y.; Burova, T. V.; Tolstoguzov, V. B. Calorimetric study of interaction of ovalbumin with vanillin. *Food Hydrocolloids* **2002**, *16*, 333–343.
(40) Pozo-Bayon, M. A.; Ruiz-Rodriguez, A.; Pernin, K.; Cayot, N. Influence of eggs on the aroma composition of a sponge cake and on the aroma release in model studies on flavoured sponge cakes. *J. Agric. Food Chem.* **2007**, *11*, 27–34.

Received for review January 23, 2008. Revised manuscript received May 7, 2008. Accepted May 18, 2008. We thank the French Ministry of Research for the CANAL-ARLE funding and the European Commission for the Marie-Curie postdoctoral fellowship to M.-A.P.-B.

JF800242R